

Reduced Complexity Neural Network Equalizers for Two-dimensional Magnetic Recording

1st Ahmed Aboutaleb

*Washington State University**

Pullman, WA 99164, USA

ahmed.aboutaleb@wsu.edu

2nd Nitin Nangare

Marvell Semiconductor Inc.,

Santa Clara, CA 95054, USA

nitinn@marvell.com

Abstract—Recent studies show promising performance gains achieved by non-linear equalization using neural networks (NNs) over traditional linear equalization in two-dimensional magnetic recording (TDMR) channels. But the examined neural network architectures entail much higher implementation complexities compared with the linear equalizer, which precludes practical implementation. For example, among the low complexity reported architectures, the multilayer perceptron (MLP) requires about 6.6 times increase in complexity over the linear equalizer. This paper investigates candidate reduced complexity neural network architectures for equalization over TDMR. We test the performance on readback signals measured over an actual hard disk drive with TDMR technology. Four variants of a reduced complexity MLP (RC-MLP) architecture are proposed. A proposed variant achieves the best balance between performance and complexity. This architecture consists of finite-impulse response filters, a non-linear activation, and a hidden delay line. The complexity of the architecture is only 1.59 times the linear equalizer’s complexity, while achieving most of the performance gains of the MLP.

Index Terms—Two-dimensional magnetic recording, neural network, equalization, reduced complexity, hard disk drive, digital storage, Viterbi algorithm

I. INTRODUCTION

The information areal density of hard disk drives (HDDs) is expected to continue increasing, while remaining cost competitive. HDDs rely on the magnetic recording channel for digital storage. Conventional one-dimensional magnetic recording (1DMR) channels store bits along one track with enough spacing between tracks to prevent inter-track interference (ITI). To increase areal density, two-dimensional magnetic recording (TDMR) decreases the cross-track spacing, resulting in significant ITI in the readback waveforms [1]. To potentially compensate for the increased ITI, the current implementation of TDMR uses two read heads positioned in the HDD reader to capture the ITI from adjacent tracks.

The readback waveforms observed by the reader are passed through a low-pass anti-aliasing filter. The output is sampled at an appropriate rate to provide the readback analog-to-digital converter (ADC) discrete-time samples. The inter-symbol interference (ISI) in the ADC samples spans many bits in the down-track direction. For maximum likelihood (ML) detection of the written bits, the Viterbi algorithm (VA) is used. The number of trellis states assumed by the VA is exponential in the length of the ISI, and the number of computations per

bit estimate is directly proportional to the number of trellis states. In TDMR, the large number of trellis states due to the 2D-ISI/ITI results in impractical complexity for ML detection.

Furthermore, for optimality in the ML sense, the canonical VA assumes that the noise is Gaussian and the 2D-ISI/ITI is linear in the coded bits. Both assumptions are not generally true in practice. Indeed, the readback waveforms suffer from non-linear impairments such as partial erasures, non-linear ISI/ITI, jitter noise, and asymmetry [2], [3]. To shorten the ISI/ITI, the typical data recovery system uses the 2D-linear minimum mean squared error (2D-LMMSE) equalizer followed by the VA detector [2], [3]. The 2D-LMMSE is realized as a finite impulse response (FIR) filter for simplicity of implementation. The equalizer’s output is then passed to the VA for ML detection. Hence, ideally, the number of trellis states needed by the VA to recover the data from the equalizer’s output is manageable. But the 2D-LMMSE equalizer is optimal in terms of the mean-squared error (MSE) only when the noise is Gaussian and the channel is linear [4]. Hence, an equalizer trained to minimize the MSE may not lead to the optimal detector bit error rate (BER), which is the desired figure of merit. Furthermore, as the areal density of the storage channel increases, non-linear impairments become more severe. Hence, the actual channel conditions deviate significantly from the optimality requirements.

Compared with conventional equalizers and detection systems, neural networks (NNs) have been shown to compensate better for the non-linear impairments in high density magnetic recording channels with significant improvement in the overall system performance for 1DMR in [2], TDMR in [3], [5]–[7], and multilayer magnetic recording (MLMR) in [8].

In [2], Nair and Moon propose using the multilayer perceptron (MLP) as an equalizer for high density 1DMR channels. Their results show that, as a non-linear equalizer, the MLP outperforms the conventional linear equalizer in terms of the MSE and BER. In [6], Sayyafan *et al.* suggest integrating a convolutional NN (CNN) with the Bahl–Cocke–Jelinek–Raviv (BCJR) to iteratively estimate and cancel the non-linear media noise. The proposed system achieves significant information density gains over competing non-NN-based system for 1DMR and TDMR channels. In [7], Luo *et al.* investigate the performance of a NN equalizer and show that it achieves lower BERs than the 2D-LMMSE over a TDMR channel. In addition, for

*Work was completed while the author was with Marvell.

application in TDMR, in [5], Shen *et al.* propose a detection system consisting of a 2D-LMMSE followed by a CNN detector. In [8], Aboutaleb *et al.* propose CNN-based systems for detection and equalization in MLMR channels with severe non-linear distortions. In [3], Shen and Nangare propose an NN equalizer followed by a VA, where the NN's parameters adapt to minimize the cross-entropy (CE). Therein, the authors show that adapting the equalizer's parameters to minimize the CE loss results lower detector BERs compared with MSE adaptation. Also, their study further confirms that the non-linear impairments are better handled using an NN equalizer.

Despite the improvements in performance reported in [5]–[8], the mentioned NN-based equalizers are much more complex than the linear equalizer baseline. Indeed, the high complexity of NN-based methods precludes practical implementation. For example, among the lowest complexity NN equalizers proposed by previous studies, the complexity of the MLP in [3] is about $6.6 \times$ the complexity of the 2D-LMMSE. To facilitate practical implementation, we propose four variants of a reduced complexity MLP (RC-MLP) architecture. RC-MLP consists of FIR filters and non-linear activations; both components can be easily realized in practice. We show that the RC-MLP architectures offer an excellent balance between performance and complexity. Among the proposed variants, an architecture achieves the best trade-off between performance and complexity. This non-linear equalizer is comprised of FIR filters and a non-linear activation function.

Furthermore, the reported results in previous studies assume synthesized data. Although advanced synthesis methods provide accurate data sets, such as the grain flipping probability model [9], [10], we examine the performance of NN-based methods on actual HDD waveforms. The novel contributions of this paper are summarized as follows.

- 1) We investigate reduced complexity neural network architectures for equalization over TDMR channels. We propose four variants of RC-MLP that achieve most of the performance gains achieved by the high complexity and high performance MLP.
- 2) We consider candidate radial basis function neural network (RBFNN)-based equalizer architectures. We compare the performance and complexities of these architectures with MLP and RC-MLP.
- 3) We test the performance of the proposed architectures and baseline methods using actual HDD data and read-back waveforms. The data is obtained from an HDD with TDMR technology. We show the balance between performance and complexity for each method. Then, we identify the architecture with the best performance-complexity balance.

II. CHANNEL MODEL AND SYSTEM OVERVIEW

This paper uses actual HDD waveforms for testing. We summarize a channel model that approximates the TDMR channel, where details can be found in [3, Sec. II] and [11]. The magnetic recording channel is a binary input, 2D ISI/ITI

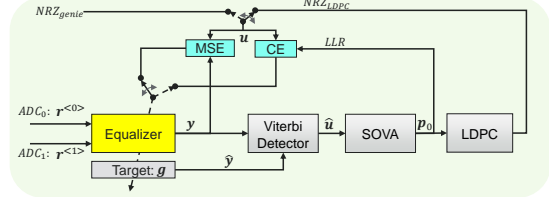


Fig. 1: Equalizer-detector system. The equalizer accepts the readback ADC samples and outputs the PR signal y . The Viterbi detector along with the SOVA compute the soft-bit estimate p_0 .

channel with non-linear distortions, correlated media noise, and additive white Gaussian noise (AWGN).

Let $\mathbf{u} = [u_n] \in \{-1, +1\}$ be a binary input sequence to be written on the media. Define the transition sequence \mathbf{b} such that $b_n \triangleq (u_n - u_{n-1})/2$. Let $h(t, w)$ denote the 2D channel response, modeled using the $\text{erf}(\cdot)$ function as in [3], [11], [12]. Then, $r_a(t)$ the continuous-time readback waveform is given by:

$$r_a(t) = \sum_{m,n} b_n h(t - nT + \Delta t_n, w + \Delta w_n) + n(t), \quad (1)$$

where T is the symbol interval, Δt_n is the down-track jitter noise, modeled as a Gaussian random process using a truncated Gaussian distribution such that $\Delta t_n < T/2$, Δw_n is the cross-track jitter noise, and $n(t)$ is the AWGN, which models the reader electronics noise.

Let $p(t, w) \triangleq h(t, w) - h(t - T, w)$ denote the channel response. Then, as detailed in [3], the equivalent discrete-time channel model is given by:

$$r_n^{(l)} = (\mathbf{p}^{(l)} * \mathbf{u})_n + n_n^{(l)}, \quad l = 0, 1, \quad (2)$$

where $\mathbf{p}^{(l)}$ is the 2D response for reader l .

Fig. 1 shows the equalizer-detector system. The equalizer processes the ADC samples from the readers. The equalizer's output is passed to the SOVA detector [13], which computes soft bit estimates as LLRs. The LLRs are then fed to the LDPC decoder to recover the information bits. The equalizer's adaptable parameters and target are adjusted using the MSE or the CE criteria.

III. ADAPTATION

A. Mean-Squared Error

Let the equalizer's output be denoted by y_n and the noise-free partial response (PR) target signal by \hat{y}_n . The equalizer output y_n depends on the equalizer's architecture design and its learnable parameters, which include the weights \mathcal{W} and biases \mathcal{B} . The equalizer's design is discussed in Sections IV and V. The noise-free PR signal is given by:

$$\hat{y}_n = (\mathbf{g} * \mathbf{u})_n, \quad (3)$$

where $*$ denotes 2D discrete-time convolution, \mathbf{g} represents the PR target, and \mathbf{u} represents the written bit sequence. For a length- N minibatch, the average MSE J_{MSE} is computed as:

$$J_{\text{MSE}} = \frac{1}{N} \sum_{n=0}^{N-1} (\hat{y}_n - y_n)^2. \quad (4)$$

For MSE adaptation, the optimization problem is given by:

$$\arg_{\mathcal{W}, \mathcal{B}, \mathbf{g}} J_{\text{MSE}} \quad (5a)$$

$$\text{subject to } \mathbf{u}^T \mathbf{g} = 1, \quad (5b)$$

where (5b) is the monic constraint (MC) on the target which sets the first tap of the target to one, i.e., $\mathbf{u} = [1, 0, 0, \dots]$. In MSE adaptation, including the MC prevents the target coefficients from converging to the trivial solution of $\mathbf{g} = 0$ and has been shown to improve the BER performance [14].

B. Cross-Entropy

Consider estimating the n th bit u_n . Its estimate is denoted by \hat{u}_n . For CE adaptation, \hat{u}_n is obtained by passing the equalizer's output to the VA and computing the soft decisions, in the form of log-likelihood ratios (LLRs), using the soft output VA (SOVA) [13]. Let $\mathbb{1}_{u_n=i}$ denote the indicator function such that $\mathbb{1}_{u_n=i} = 1$ if $u_n = i$, $i \in \{0, 1\}$ (and zero otherwise), and define $p_{0,n} \triangleq \Pr\{\hat{u}_n = 0\}$. Then, for the n th bit, the CE loss is computed as:

$$\mathcal{H}\{u_n, \hat{u}_n\} = -\mathbb{1}_{u_n=0} \log(p_{0,n}) - \mathbb{1}_{u_n=1} \log(1 - p_{0,n}). \quad (6)$$

The procedure in [3] is followed to compute $p_{0,n}$ from the LLR. The objective function to minimize is the average CE loss computed over a minibatch of length N as:

$$J_{\text{CE}} = \frac{1}{N} \sum_{k=0}^{N-1} \mathcal{H}\{u_n, \hat{u}_n\}. \quad (7)$$

Hence, the optimization problem can be written as:

$$\underset{\mathcal{W}, \mathcal{B}, \mathbf{g}}{\text{minimize}} \quad J_{\text{CE}}. \quad (8)$$

The optimization problems in (5) and (8) are solved numerically using the back-propagation algorithm with stochastic gradient descent (SGD) [15, Ch. 8].

Adapting the equalizer's parameters using the CE criterion is equivalent to maximum likelihood adaptation since the BER and soft-bit information are jointly improved. Thus, for any equalizer structure CE adaptation outperforms MSE adaptation in terms of BER [3].

IV. NEURAL NETWORK-BASED EQUALIZERS

A. Multilayer Perceptron

Fig. 2 shows the architecture of the MLP equalizer. To estimate the n th bit in the downtrack direction, the MLP uses the ADC samples observed over a sliding window of size $2M + 1$ for each reader centered around the n th readback sample. Let $\mathbf{r}_n \triangleq [\mathbf{r}_n^{(0)}, \mathbf{r}_n^{(1)}]$ denote such ADC samples from the TDMR reader centered around the n th sample,

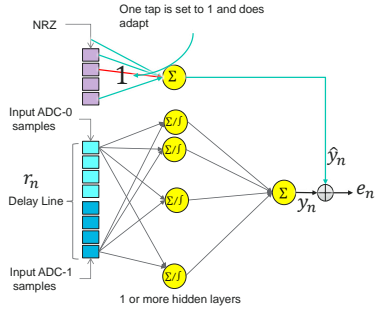


Fig. 2: Multilayer perceptron (MLP). The inputs are delayed ADC samples over a sliding window. The connections here represent a fully connected layer consisting of a matrix with dimensions consistent with the input length and the designed number of hidden outputs. The final equalizer output is an affine combination of all hidden outputs.

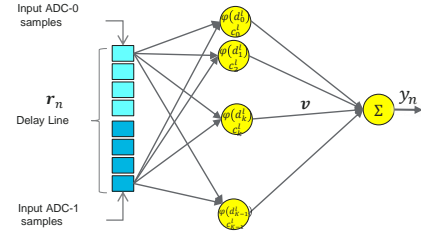


Fig. 3: Radial basis function neural network (RBFNN). The readback samples are used to compute the distances $d_k^l = \|\mathbf{r}_{n,\text{vec}} - \mathbf{c}_k^l\|$. A basis function $\phi(\cdot)$ is applied on the hidden outputs.

where the ADC samples per reader are defined as: $\mathbf{r}_n^{(l)} \triangleq [r_{n-M}^{(l)}, r_{n-1}^{(l)}, \dots, r_n^{(l)}, r_{n+1}^{(l)}, \dots, r_{n+M}^{(l)}]^T$, $l = 0, 1$. The MLP contains a matrix of weights $\mathbf{W} = [w_{i,j}] \in \mathbb{R}^{(4M+2) \times K}$ that multiplies the vectorized input samples $\mathbf{r}_{n,\text{vec}} = \text{vec}(\mathbf{r}_n)$ to provide K intermediate outputs. After adding the biases $b_{0,k}$, $k = 1, \dots, K$, to the intermediate outputs, the hidden outputs are obtained by applying an element-wise non-linear activation function $\Psi(\cdot)$ to the outcome. Examples of $\Psi(\cdot)$ include the hyperbolic tangent, the sigmoid, and rectified linear units (ReLU) activations. The MLP output is an affine combination of the K hidden outputs, where $\mathbf{v} = [v_j] \in \mathbb{R}^K$ is the vector of coefficients used in the linear combination and b_2 is the added bias term. More precisely, the output of the MLP is given by:

$$y_n = \sum_{j=0}^{K-1} v_j \Psi \left(\sum_{i=0}^{4M+1} w_{i,j} \mathbf{r}_{n,\text{vec},i} + b_{0,j} \right) + b_1. \quad (9)$$

The learnable parameters for the MLP are the weights and biases $\mathcal{W} = \{\mathbf{W}, \mathbf{v}\}$ and $\mathcal{B} = \{b_{0,k}\}_{k=0}^{K-1}, b_1\}$, respectively. Hence, the total number of parameters for the MLP is $|\mathcal{W}| + |\mathcal{B}| = 4MK + 4K + 1$. From (9), for each output, implementing the MLP requires $4MK + 3K$ multiplications and additions, and K evaluations of $\Psi(\cdot)$.

B. Radial Basis Function Neural Network

Fig. 3 shows the architecture of the RBFNN. The RBFNN replaces the matrix multiplication and non-linear activation in the MLP with distances from cluster centroids and a basis

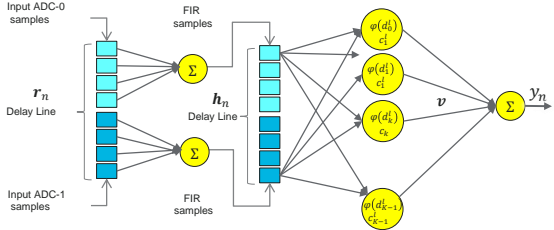


Fig. 4: Finite impulse response-radial basis function neural network (FIR-RBFNN). Two FIR filters reduce the input dimension so that the centers c_k^l lie in a lower dimensional space compared with the readings r_n , thereby reducing the overall complexity.

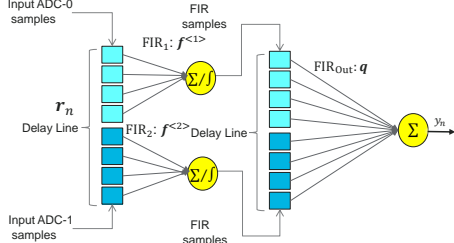


Fig. 5: RC-MLP1 architecture.

function, respectively. The RBFNN is characterized by the centroids c_k with K biases $b_{1,k}$, $k = 1, \dots, K$, a length- K vector v with bias b_2 , a norm $\|\cdot\|$, typically the Euclidean norm, and a basis function $\phi(\cdot)$. The length of the centroids c_k matches the number of the input samples. The canonical implementation of the RBFNN uses the Euclidean distance. Given an input instance, the distance between the input samples vectors and centroids is computed. Then, the basis function is applied to the distances to provide the hidden output. Finally, the RBFNN output is computed as an affine combination of the hidden outputs. More specifically, the RBFNN output is described by:

$$y_n = \sum_{k=0}^{K-1} v_k \phi(\|\mathbf{r}_{n,\text{vec}} - \mathbf{c}_k\| + b_{0,k}) + b_1, \quad (10)$$

where $\mathbf{c}_k \in \mathbb{R}^{4M+2}$. To reduce the dimension of the centroids, we can use centroids that have the same length as the number of ADC samples per reader, instead of the vectorized ADC samples for both readers. If K is even, then this formulation gives the output of the RBFNN as:

$$y_n = \sum_{l=0}^1 \sum_{k=0}^{K/2-1} v_k \phi(\|\mathbf{r}_n^{(l)} - \mathbf{c}_k^l\| + b_{l,k}) + b_l, \quad (11)$$

where $\mathbf{c}_k^l \in \mathbb{R}^{2M+1}$. In (11), $K/2$ centroids are assigned for each ADC sequence. The learnable parameters consist of the centers $\mathcal{C} = \{\mathbf{c}_k\}_{k=0}^{K-1}$, weights vector v , and biases $\mathcal{B} = \{\{b_{l,k}\}_{k=0}^{K-1}, b_l\}_{l=0}^1$. Thus, the RBFNN uses $|\mathcal{C}| + |\mathcal{V}| + |\mathcal{B}| = 2KM + 3K + 2$ learnable parameters.

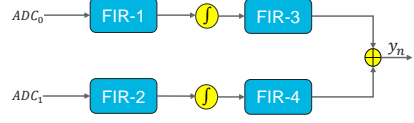


Fig. 6: FIR representation of RC-MLP1.

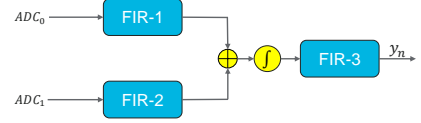


Fig. 7: RC-MLP2.

V. PROPOSED REDUCED COMPLEXITY NEURAL NETWORK-BASED EQUALIZERS

A. FIR-RBFNN

To decrease the complexity of the RBFNN, we introduce an FIR filter $\mathbf{f}^{(l)} \in \mathbb{R}^{2P+1}$, $l = 0, 1$, per ADC sequence, that interfaces the two input ADC sequences, as shown in Fig. 4. The FIR filter maps the length- $(2M+1)$ ADC input to a length- $(2M'+1)$ sequence, where $M' < M$. The FIR-RBFNN output is given by:

$$y_n = \sum_{l=0}^1 \sum_{k=0}^{K/2-1} v_k \phi(\|(\mathbf{f}^{(l)} * \mathbf{r}_n^{(l)}) - \mathbf{c}_k^l\| + b_{l,k}) + b_l, \quad (12)$$

where the dimension of the centroids is now $2M'+1$.

B. RC-MLP

We propose four variants of reduced complexity MLP (RC-MLP) architectures. RC-MLP1 uses FIR filters to implement the matrix multiplication and affine combination operations in MLP, resulting in a lower complexity architecture. Two FIR filters, FIR-1 and FIR-2, are introduced at the input layer – one filter per ADC stream. After applying a non-linear activation, the hidden outputs corresponding to each filter are then stacked in one or two delay lines, depending on the specific architecture as shown in Fig. 5 and 6.

1) *RC-MLP1*: Fig. 5 shows the architecture of RC-MLP1. Two intermediary delay lines are introduced to store temporary hidden outcomes from FIR-1 and FIR-2 separately. The last layer consists of two FIR filters, FIR-3 and FIR-4, that map the delayed hidden samples to the final output.

Let $\mathbf{f}^{(l)}$ and $\mathbf{q}^{(l)}$, $l = 0, 1$, denote the FIR filters interfacing the input ADC samples and hidden delayed outputs, respectively. The lengths of $\mathbf{f}^{(l)}$ and $\mathbf{q}^{(l)}$ are $2M+1$ and K , respectively, where K is the number of hidden delay samples per ADC path. Then, the equalizer output y_n is given in terms of the hidden outputs $h_n^{(l)}$ as:

$$h_n^{(l)} = \Psi((\mathbf{f}^{(l)} * \mathbf{r}_n^{(l)})_n + b_{0,l}) \quad (13)$$

$$y_n = \sum_{l=0}^1 (\mathbf{q}^{(l)} * h_n^{(l)})_n + b_1, \quad (14)$$

where $b_{0,l}$ and b_1 are bias terms. RC-MLP1 uses $4M+2K+7$ learnable parameters and requires $4M+2K+2$ multipliers and two evaluations of $\psi(\cdot)$ per bit estimate.

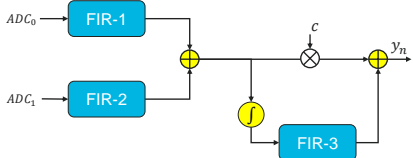


Fig. 8: RC-MLP3.

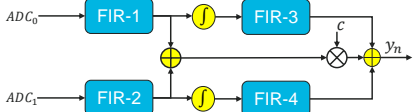


Fig. 9: RC-MLP4.

2) *RC-MLP2*: In RC-MLP2, FIR-1's and FIR-2's outputs are summed. Then, a non-linear activation function is applied to the summation. Hence, only one hidden delay line is needed with K samples. FIR-3 interfaces the hidden delay line to provide the equalizer output. The hidden outputs and equalizer output can be expressed as:

$$h_n = \Psi \left(\sum_{l=0}^1 (\mathbf{f}^{(i)} * \mathbf{r}_n^{(i)})_n + b_0 \right) \quad (15)$$

$$y_n = (\mathbf{q} * \mathbf{h}_n)_n + b_1. \quad (16)$$

RC-MLP2 requires $4M + K + 4$ parameters, $4M + K$ multipliers, and one evaluation of $\psi(\cdot)$ per bit estimate.

3) *RC-MLP3*: RC-MLP3 adds a linear connection from the input to the output in the RC-MLP2 structure as shown in Fig. 8. The motivation for adding the linear connection is to jump start the system using the FIR-1 and FIR-2 combination as a linear equalizer, while maintaining the improved generalization afforded by the non-linear NN equalizer. Furthermore, including this direct connection between the first hidden output to the final output provides a more direct path for error propagation from the output to adapting FIR-1 and FIR-2. The equalizer's output for RC-MLP3 can be written as:

$$h_n, \text{Linear} = \sum_{l=0}^1 (\mathbf{f}^{(i)} * \mathbf{r}_n^{(i)})_n + b_0, \quad (17)$$

$$h_n = \Psi(h_n, \text{Linear}), \quad (18)$$

$$y_n = (\mathbf{q} * \mathbf{h}_n)_n + ch_n, \text{Linear} + b_1. \quad (19)$$

4) *RC-MLP4*: RC-MLP4 adds a linear connection to RC-MLP1 as shown in Fig. 9. The output is given by:

$$h_n^{(l)}, \text{Linear} = \sum_{l=0}^1 (\mathbf{f}^{(i)} * \mathbf{r}_n^{(i)})_n + b_{0,l}, \quad (20)$$

$$h_n^{(l)} = \Psi(h_n^{(l)}, \text{Linear}), \quad (21)$$

$$y_n = \left(\sum_{l=0}^1 \mathbf{q}^{(l)} * \mathbf{h}_n^{(l)} \right)_n + ch_n, \text{Linear} + b_1. \quad (22)$$

TABLE I: Performance and complexity comparison. The BER is computed over the first 20 sectors.

Architecture	K	BER	Complexity
2D-LMMSE with fixed [3,7,1] target	N/A	0.027982	22
2D-LMMSE	N/A	0.025548	22
2D-LECE	N/A	0.023066	22
2D-LECE with 21 Taps per ADC	N/A	0.022658	42
RBFNN	6	0.02315	157
RBFNN	20	0.021608	521
RBFNN	30	0.021733	781
FIR-RBFNN, Gaussian Basis	6	0.021860	107
FIR RBFNN, Tanh Basis	6	0.022497	107
RC-FIR-RBFNN, Linear Basis	6	0.022773	41
RC-FIR-RBFNN, Gaussian Basis	6	0.023744	41
MLP	6	0.020757	145
RC-MLP1	6	0.022736	31
RC-MLP1	10	0.022048	35
RC-MLP1	14	0.021916	39
RC-MLP1	18	0.021862	43
RC-MLP2	9	0.021668	34
RC-MLP3	9	0.021243	35
RC-MLP4	18	0.021367	44

VI. NUMERICAL RESULTS

A. Setup

We test the discussed architectures on raw ADC samples obtained from an HDD with TDMR technology. The data consists of 520 sectors, where each sector contains $N = 39,268$ bits. Two ADC samples per bit are available via the TDMR read head. The CTS is 52%, and the track pitch is 85 nm.

B. Linear Equalizers

Table I shows the BER performance and complexity of the discussed methods evaluated on the first 20 sectors. All equalizers are adapted based on the CE criterion except the 2D-LMMSE. The linear equalizer uses 11 taps per ADC sequence except when noted. Computational complexity here is measured as the number of learnable parameters required by the method. The number of parameters is directly proportional to the number of FLOPs required per estimation. The baseline method used in practice is the 2D-LMMSE equalizer. In all experiments, the target coefficients adapt to minimize the objective function under the monic constraint. The exception is an experiment where the target is fixed to [3, 7, 1] and the 2D-LMMSE is used. This configuration is a baseline that is often used in practice. Adapting the target reduces the BER by 8.70% when the MSE is used as the adaptation criterion. Adapting the linear equalizer with CE instead of the MSE results in further reduction of the BER by about 12.67%. A further BER improvement of the linear equalizer by about 1.77% is achieved by increasing the number of FIR taps to 21 per ADC sequence. With 21 taps per ADC, the linear equalizer's complexity increases by about 90%.

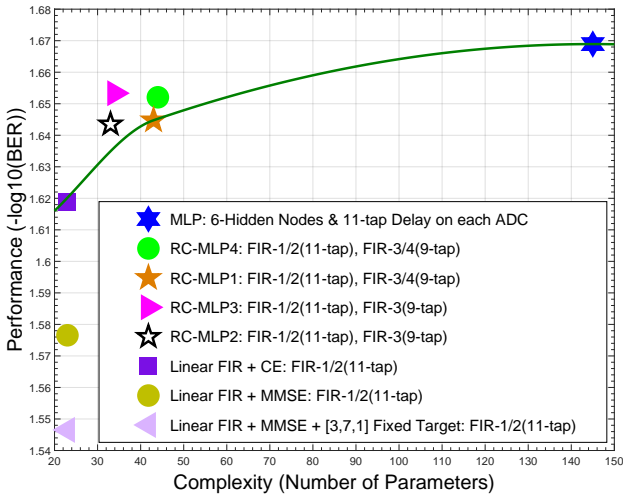


Fig. 10: Performance versus complexity for 520 sectors.

C. RBFNN-based Equalizers

The basic RBFNN equalizer increases complexity without significant improvement in the BER even with 20 and 30 cluster centroids per ADC. To improve the performance, FIR-RBFNN is used. The two FIR filters, one per ADC sequence, interface the ADC samples and map the 11 samples per ADC to 5 samples per ADC. In this case, the centroids lie in 5 dimensional space (instead of 11), making the distance computation more efficient. This FIR-RBFNN architecture with 6 centroids per ADC achieves BER performance that is only 1.67% higher than the RBFNN with 20 centroids, while requiring about 4.87 less complexity. Nonetheless, FIR-RBFNN's BER is 5.23% lower than 2D linear equalizer with cross-entropy (2D-LECE), but its complexity is about 4.86 higher. RC-FIR-RBFNN decreases complexity by about 37% over FIR-RBFNN. With linear basis, RC-FIR-RBFNN achieves a similar BER.

D. RC-MLP

The MLP with 6 hidden nodes achieves the lowest BER, which is 10% lower than the 2D-LECE with 11 taps, while demanding a $6.6\times$ increase in complexity. In comparison, RC-MLP1 with 6 hidden nodes achieves a BER performance that is 5.22% lower than the 2D-LECE with only a $1.95\times$ complexity increase. RC-MLP2 achieves a 6.06% lower BER compared with 2D-LECE while requiring only a $1.54\times$ increase in complexity. RC-MLP3 achieves a BER reduction of 7.9% with a complexity increase of $1.59\times$ over 2D-LECE. RC-MLP4 achieves 7.37% lower BER with a $2\times$ increase in complexity. Thus, RC-MLP3 achieves the best balance between complexity and performance improvement. Also, RC-MLP3 decreases the implementation complexity by about $4.14\times$ compared with the MLP. Furthermore, RC-MLP3 achieves 24.08% and 16.85% reductions in the BER compared with 2D-LMMSE with fixed and adapting targets, respectively. Fig. 10 summarizes the performance complexity trade-off.

VII. CONCLUSION

We examine the performance-complexity trade-off for different equalizer architectures. The multilayer perceptron (MLP) achieves significant performance gains over the linear equalizer. But its complexity is about $6.6\times$ the complexity of the linear equalizer. To enable practical implementation of non-linear neural network equalizer, four variants of a reduced complexity MLP (RC-MLP) are proposed. Among them, an architecture, named RC-MLP3, outperforms its variants and achieves most of the performance gains of the MLP, while requiring only $1.59\times$ the complexity of the linear equalizer. If L and K are the lengths of the input and hidden output, respectively, then the complexities of MLP and RC-MLP scale as $O(LK + K)$ and $O(L + K)$, respectively.

REFERENCES

- [1] R. Wood, M. Williams, A. Kavcic, and J. Miles, "The feasibility of magnetic recording at 10 terabits per square inch on conventional media," *IEEE Transactions on Magnetics*, vol. 45, no. 2, pp. 917–923, 2009.
- [2] S. K. Nair and J. Moon, "Data storage channel equalization using neural networks," *IEEE Transactions on Neural Networks*, vol. 8, no. 5, pp. 1037–1048, 1997.
- [3] J. Shen and N. Nangare, "Nonlinear equalization for TDMR channels using neural networks," *2020 54th Annual Conference on Information Sciences and Systems (CISS)*, pp. 1–6, 2020.
- [4] J. M. Mendel, *Lessons in estimation theory for signal processing, communications, and control*. Pearson Education, 1995.
- [5] J. Shen, A. Aboutaleb, K. Sivakumar, B. J. Belzer, K. S. Chan, and A. James, "Deep neural network a posteriori probability detector for two-dimensional magnetic recording," *IEEE Transactions on Magnetics*, vol. 56, no. 6, pp. 1–12, 2020.
- [6] A. Sayyafan, B. J. Belzer, K. Sivakumar, J. Shen, K. S. Chan, and A. James, "Deep neural network based media noise predictors for use in high-density magnetic recording turbo-detectors," *IEEE Transactions on Magnetics*, vol. 55, no. 12, pp. 1–6, 2019.
- [7] K. Luo, S. Wang, K. S. Chan, W. Chen, J. Chen, P. Lu, and W. Cheng, "A study on block-based neural network equalization in TDMR system with LDPC coding," *IEEE Transactions on Magnetics*, vol. 55, no. 11, pp. 1–5, 2019.
- [8] A. Aboutaleb, A. Sayyafan, K. Sivakumar, B. Belzer, S. Greaves, K. S. Chan, and R. Wood, "Deep neural network-based detection and partial response equalization for multilayer magnetic recording," *IEEE Transactions on Magnetics*, pp. 1–1, 2020.
- [9] K. S. Chan, R. Radhakrishnan, K. Eason, M. R. Elidrissi, J. J. Miles, B. Vasic, and A. R. Krishnan, "Channel models and detectors for two-dimensional magnetic recording," *IEEE Transactions on Magnetics*, vol. 46, no. 3, pp. 804–811, 2010.
- [10] S. J. Greaves, K. S. Chan, and Y. Kanai, "Areal density capability of dual-structure media for microwave-assisted magnetic recording," *IEEE Transactions on Magnetics*, vol. 55, no. 12, pp. 1–9, 2019.
- [11] R. Pighi, R. Raheli, and U. Amadei, "Multidimensional signal processing and detection for storage systems with data-dependent transition noise," *IEEE Transactions on Magnetics*, vol. 42, no. 7, pp. 1905–1916, 2006.
- [12] P. Kovintavewat, I. Ozgunes, E. Kurtas, J. R. Barry, and S. W. McLaughlin, "Generalized partial-response targets for perpendicular recording with jitter noise," *IEEE Transactions on Magnetics*, vol. 38, no. 5, pp. 2340–2342, 2002.
- [13] J. Hagenauer and P. Hoeher, "A Viterbi algorithm with soft-decision outputs and its applications," in *1989 IEEE Global Telecommunications Conference and Exhibition 'Communications Technology for the 1990s and Beyond'*, 1989, pp. 1680–1686 vol.3.
- [14] Jackyun Moon and Weining Zeng, "Equalization for maximum likelihood detectors," *IEEE Transactions on Magnetics*, vol. 31, no. 2, pp. 1083–1088, 1995.
- [15] I. Goodfellow, Y. Bengio, A. Courville, and Y. Bengio, *Deep learning*. MIT press Cambridge, 2016, vol. 1.